Schweizerische Eidgenossenschaft
Confédération suisse
Confederazione Svizzera
Confederaziun svizra

Federal Department of the Environment, Transport, Energy and Communications DETEC

Swiss Federal Office of Energy SFOE
Energy Research and Cleantech Division

Final report dated 9th of November 2021

Transparent nanomeshes for smart windows

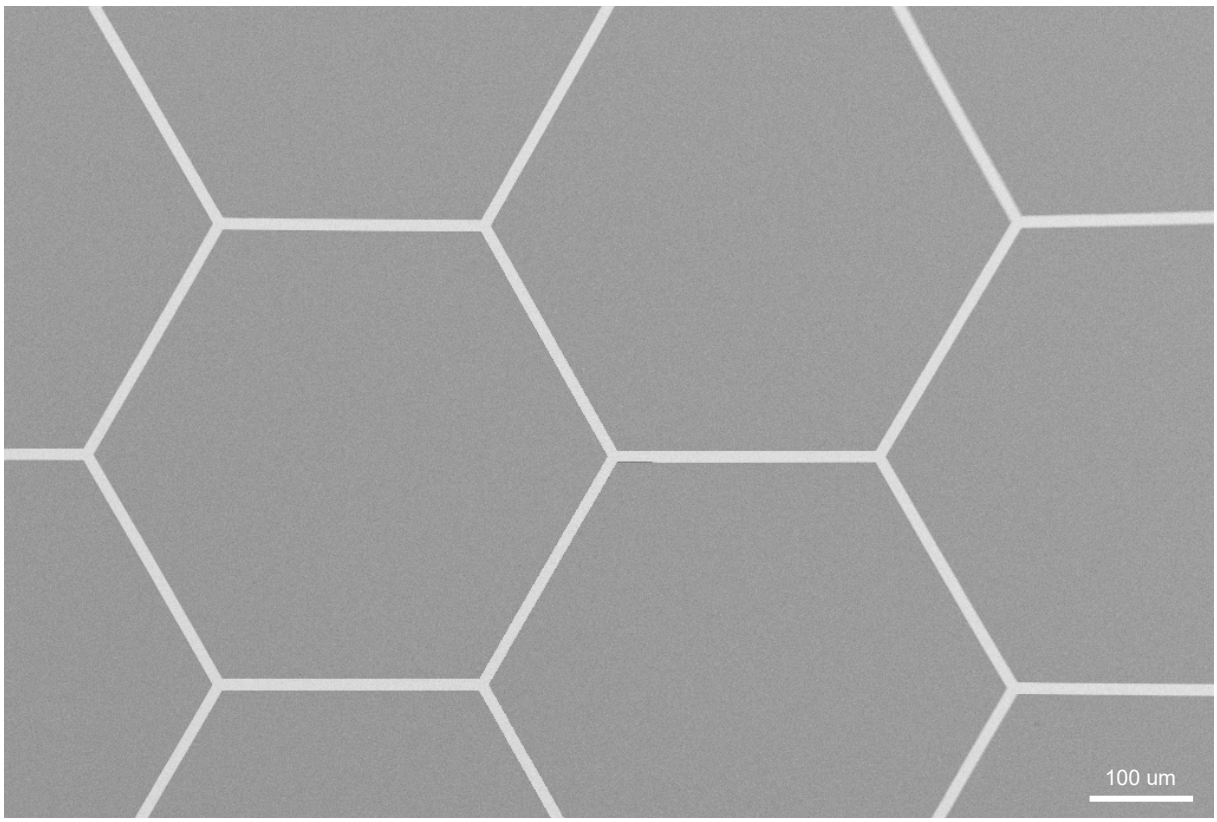

SEM image of a silver honeycomb nanomesh-structure made by photolithography

Date: 9th of November 2021

Location: Bern

Publisher:
Swiss Federal Office of Energy SFOE
Energy Research and Cleantech
CH-3003 Bern
www.bfe.admin.ch

Subsidy recipients:
École Polytechnique Fédérale de Lausanne **EPFL**
Solar Energy and building Physics Laboratory LESO-PB
CH-1003 Lausanne
https://www.epfl.ch/labs/leso/research/domains/nano_solar_conversion/

Authors:
Jeremy Fleury, EPFL/LESO-PB, jeremy.fleury@epfl.ch
Dr. Andreas Schüler, EPFL/LESO-PB, andreas.schueler@epfl.ch

SFOE project coordinators:
Andreas Eckmanns, andreas.eckmanns@bfe.admin.ch

SFOE project manager:
Nadège Vetterli, nadege.vetterli@anex.ch

SFOE contract number: SI/501818-01

Summary

Conventional selective **low-e coatings for windows** of residential buildings have a cut-off frequency in the near infrared spectral region NIR, limiting the resulting solar heat gain coefficient to g ≈ 0.5. By structuring the coating into nanomeshes, the selectivity shall be enhanced, and higher solar heat gains shall be achieved. The resulting increase in solar heat gains will lead to **energy savings in heating** in the residential sector. In addition to this, metal nanomeshes will also allow to replace the transparent conductive oxide layer in **electrochromic windows**, reducing the needs for indium, and leading to **higher switching speed and switching homogeneity**.

Résumé

Les vitrages isolants **avec revêtements basse émissivité** pour les bâtiments résidentiels agissent comme un miroir thermique pour les ondes du proche infrarouge (IR) ce qui améliore l'isolation mais limite aussi les gains solaires thermiques (valeur g ≈ 0.5). Une sélectivité dans la région du spectre IR peut être réalisée en structurant le revêtement dans l'échelle nanométrique. Ces « nanomesh » permettent d'augmenter les gains solaires thermiques et ainsi des **économies de chauffage** en hiver. De plus, les nanomesh métalliques pourront aussi remplacer les oxides conducteurs transparents dans les **fenêtres électrochromes**, ce qui permet de réduire le besoin en indium et d'améliorer la **vitesse et l'homogénéité lors des changements de phases**.

Zusammenfassung

Konventionelle selektive **low-e Beschichtungen für Fenster** von Wohngebäuden weisen eine Übergangsfrequenz im nahen Infrarotbereich NIR auf, die den Gesamtenergiedurchlasswert auf maximal g ≈ 0.5 begrenzt. Durch Strukturierung der Beschichtung zu einem Nanogitter soll die Selektivität verstärkt und der Gesamtenergiedurchlasswert erhöht werden. Die höheren Solarenergieeinträge werden **Einsparungen der Heizenergie** im Wohnbereich möglich machen. Weiterhin werden metallische Nanogitter es möglich machen, auf die Verwendung von transparenten leitfähigen Oxiden und insbesondere Indium in **elektrochromen Fenstern** zu verzichten, die **Schaltgeschwindigkeit zu erhöhen**, und die **Homogenität der Umfärbung zu verbessern**.

Contents

Abbreviations

FSS	Frequency Selective Surface
Low-e	Low-emissivity
IR	Infrared
SHGC	Solar Heat Gain Coefficient
TCO	Transparent Conductive Oxides
ITO	Indium Tin Oxide
FTO	Fluorine Doped Tin Oxide
AZO	Al-doped Zinc Oxide
SEM	Scanning Electron Microscopy
EM	Electronmagnetic

1 Introduction

1.1 Background information and current situation

In 2017, space heating was the dominant part of Swiss energy consumption (239.2 PJ), corresponding to a share of 31.3 % of the total energy consumption (763.4 PJ) [1]. 158.9 PJ (20.8 %) are consumed for space heating in private households. In comparison, the energy for lighting and air conditioning, ventilation and cooling in the households contributed to, respectively, 4.9 PJ (0.6 %) and 4.6 PJ (0.6 %). Nowadays, the use of insulating glazing belongs to state of the art in modern buildings as well as in building retrofit. The use of low-emissivity (low-e) coatings in combination with argon filling allow decreasing the energy loss through the glazing. This results in a reduction of thermal transmittance (U-value) of double glazing from approx. 2.8 to 1.2 *W/(m^2K)* [2]. Low-e coatings are good reflectors in the mid-infrared (MIR), and therefore also poor emitters for thermal radiation. However, due to the coating, solar heat gain coefficient (SHGC, also known as g-value) is reduced from approx. g = 0.8 to g < 0.5. For highly glazed buildings, this reduction of solar gains is even desired.

However, for residential buildings with a comparably low window-to-wall ratio, a higher SHGC would be beneficial when a suitable form of solar protection such as blinds is provided. Likewise, higher solar heat gains could be achieved in winter, leading to energy savings in space heating. Therefore, it is interesting to investigate new approaches that allow an increase in solar transmittance and SHGC while maintaining a low thermal emissivity *e*. The selectivity of low-e coatings needs thus to be enhanced. With this purpose in mind, metallic nanomeshes combine interesting features such as high transparency with electrical conductivity and low thermal emissivity.

During 2017, in the services sector and agriculture, 25.7 % of the electricity consumption was used for cooling, ventilation and domestic technology and 23.8 % for lighting [1]. For highly glazed office buildings, even in Switzerland, a form of solar protection is needed to avoid excessive cooling needs and to provide thermal and visual comfort. External blinds are susceptible to mechanical failure and cannot be used in high-rise buildings. Internal blinds are much less efficient because solar energy enters the building and must be extracted. In many cases, sun protection coatings must be used. However, those limit the solar heat gains in winter. The increased use of windows with switchable solar heat gains (such as electrochromic windows) would thus limit the cooling needs in summer and decrease the heating needs in winter. For current electrochromic windows, the time for switching between the bright and colored states is in the order of 10 - 20 minutes, and the coloration and discoloration are not homogenous (starting from the edges of the panes). With a better lateral charge transport in the transparent conductive electrode, the switching speed and -homogeneity could be significantly improved.

Alternative technologies for switchable windows include liquid crystal light valves and suspended particle devices. All switchable window technologies are based on transparent conductive electrodes, which are currently made from transparent conductive oxides (TCOs). Indium tin oxide (ITO) belongs to the TCOs with the highest performance regarding the trade-off between transparency and electrical conductivity. With the widespread use of screen and display technologies and the growing market of photovoltaics, the demand for indium is constantly increasing. However, indium is one of the scarcer elements, at least in terms of average abundance in the Earth's crust (see NREL report [3]). Conductive transparent nanomeshes will also help reduce the use of TCO materials (ITO, fluorine-doped tin oxide (FTO), Al-doped zinc oxide (AZO), ...) for various optoelectronic devices such as flat panel displays (LCD), touch screen, organic light-emitting diodes (OLEDs) and photovoltaics.

1.2 Purpose of the project

This project targets to study the development of conductive transparent nanomeshes for optoelectronic applications. It will consist of a metal nanomesh with enhanced selectivity in the electromagnetic spectrum and high electrical conductivity. To achieve these goals, scientific questions about light interaction and electronic transport properties need to be investigated:

1. How do electromagnetic (EM)-waves interact with the nanomesh?

(a) Considering the wavelength range from 10^{-7} to 10^{-2} m, which physical effects depend on the wavelength of the incident EM-wave?

(b) How depend the physical observables, such as transmittance/reflectance/absorbance, on the scale and geometry of the structure?

(c) Will there be a plasmonic resonance being related to the plasma frequency of free conduction electrons?

(d) What happens if the size-dependent resonance of a frequency selective surface (FSS) is tuned to the same frequency?

2. What are the electronic transport properties of nanomeshes?

(a) For a sheet resistance (R*s*) of 10 Ohm/*sq*, what maximum visible transmittance can be achieved?

(b) Inversely, for a visible transmittance above 80 %, what minimum sheet resistance can be obtained?

(c) What are suitable hierarchical structures for lateral charge transport on the corresponding mm, *µ*m, nm-scales?

(d) How can such nanomeshes be incorporated into an electrochromic device?

1.3 Objectives

- Design of nanomeshes based on knowledge on suitable patterns, and on the knowledge on dependence of the transition frequency on mesh shape and dimensions
- Preparation of nanomeshes:
  - formation of nanomeshes in selective low-e coatings
  - fabrication of nanomeshes based on transfer of nanowire
  - fabrication of hybrid structures nanomesh/TC
- Characterization of structural, thermo-optical, and electrical properties of nanomeshes
  - Scanning tunneling microscopy STM and spectroscopy STS
  - Scanning electron microscopy SEM
  - UV/VIS/NIR transmittance
  - MIR reflectance
  - thermal emissivity
  - electrical conductivity
- Target values:
  - improvement in solar heat gain coefficient g from approx. g = 0.5 to g > 0.7
  - thermal emissivity changes below 10 percentage points (for low-e coatings)
  - Sheet resistance R_{sq} < 50 ohm/sq (for switchable windows)

2 Procedures and methodology

Our methodology included the tasks listed below where each work package is investigated in detail in the results section.

WP1: Literature study

WP2: Design of nanomeshes based on a theoretical understanding of the underlying principles

Optical selective nanomeshes have the function of a high-pass filter. Short EM-waves are transmitted, while long EM-waved are reflected. The size and the shape of the openings of the mesh determine the position of the transition frequency and were simulated based on the Maxwell's equations and a finite-difference time-domain (FDTD) solver.

WP3: Origination of micro-/nano- structures

Origination of micro-/nano- structures included laser ablation and lithography on glass. UV-photolithography was done in the Center of Micro/Nanotechnology CMI at EPFL and the laser ablation was carried out in our optical laboratory.

WP4: Replication of micro-/nano- structures

Options for replication of micro-/nano- structures include replication in PDMS, printing of a sacrificial layer and subsequent coating, as well as transfer of metal nanowires by embossing/printing.

WP5: Characterization of nanomeshes

SEM, STM, UV-VIS-NIR spectrophotometry, FTIR spectrophotometry in the MIR, IR emissiometry, electrical conductivity

WP6: Enhancing the selectivity of a low-e coating

A low-e coating with a solar energy transmission tauE < 0.5 will be structured as nanomesh. The steps of origination and replication developed in WP3 and WP4 can be used for printing a sacrificial layer before coating. The nanomesh structure will then be obtained by subsequent lift-off of sacrificial layer and coating. Another option is direct structuring of the coating by UV/e-beam lithography.

WP7: Study of hybrid structures with metal nanomeshes and thin TCO layers

Metal nanomeshes will be produced and combined with very thin film of TCO to achieve high conductivity and transparency. This hybrid structure allows for homogenous distribution of charges on the micro as well as nanoscale.

WP8: Preparation of electrochromic device with metal nanomeshes as conductive transparent layer

The hybrid nanomeshes produced in WP7 will be used as conductive transparent layer in electrochromic device which will greatly reduce the switching time and homogeneity.

WP9: Evaluation of feasibility of envisaged applications (insulating glazing with enhanced selectivity, electrochromic windows)

The feasibility and large production of the samples produce in WP6, 7, 8 will finally be assessed.

3 Results and discussion

This section presents qualitative and quantitative results, findings and experiences achieved within the framework of this project for each work package based on the research proposal.

WP1: Literature study

As mentioned in the introduction, metallic nanomeshes present interesting features such as low thermal emissivity and high transparency combined with electrical conductivity. These aspects, as well as the physical properties, the suitable choices of materials, the dimensions, and the existing methods to create nanomeshes are described in the following section.

Low-e coating with enhanced selectivity

The type of glazing required in a building for minimal energy consumption depends greatly on the climate. The diagram shown in Figure 1 depicts the performance requirement in building glazing for various climate. On one hand, in the case of hot climate, SHGC should be kept to a minimum to avoid overheating and the transmittance in the visible spectrum (T_V) should ideally stay high enough to allow adequate visual comfort. But on the other hand, for cold climate, SHGC should be kept as high as possible to increase the solar energy gain, leading to energy savings in space heating.

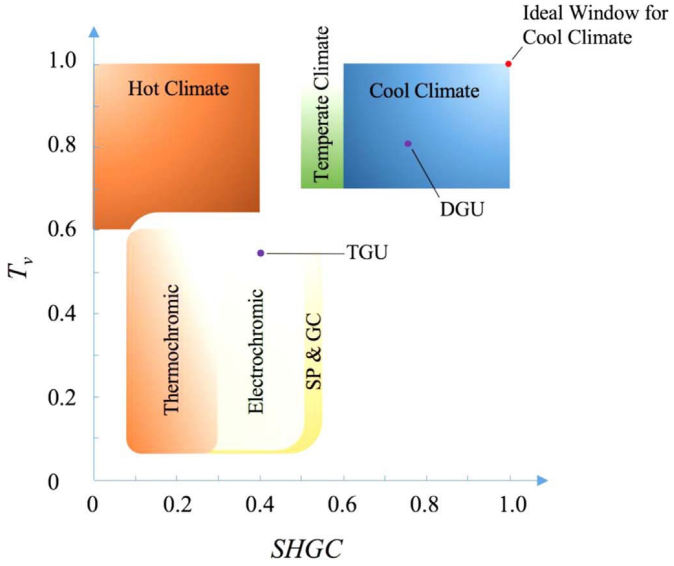

Figure 1 : Performance requirements for various climates and performance of thermochromic, electrochromic, suspended particles (SP), and gaso-chromic (GC) windows. Typical double and triple glazing units (DGU and TGU) are shown as dots. [4]

The ideal selectivity (reflection and transmission spectra) is illustrated as a plot in Figure 2. The red and blue lines give the theoretically most effective nanomesh coating that optimize the solar heat gain. This specific selectivity can be achieved by structuring the coating on the windows into nanomeshes.

The principle of selective wave propagation through the nanomesh structure is further explained in Figure 3 and work as follow: for short-wavelength radiation in the spectral range of solar radiation (VIS-NIR), the openings are comparatively large to the wavelength, and the electromagnetic wave is transmitted. Therefore, the nanomesh is transparent (see Fig. 3a). For long-wavelength radiation in the spectral range of thermal radiation, the dimensions of the openings are comparable to the wavelength, and the electromagnetic wave is reflected. Therefore, the nanomesh is an infrared-reflector and the surface with the nanomesh has a low thermal emissivity (see Fig. 3b).

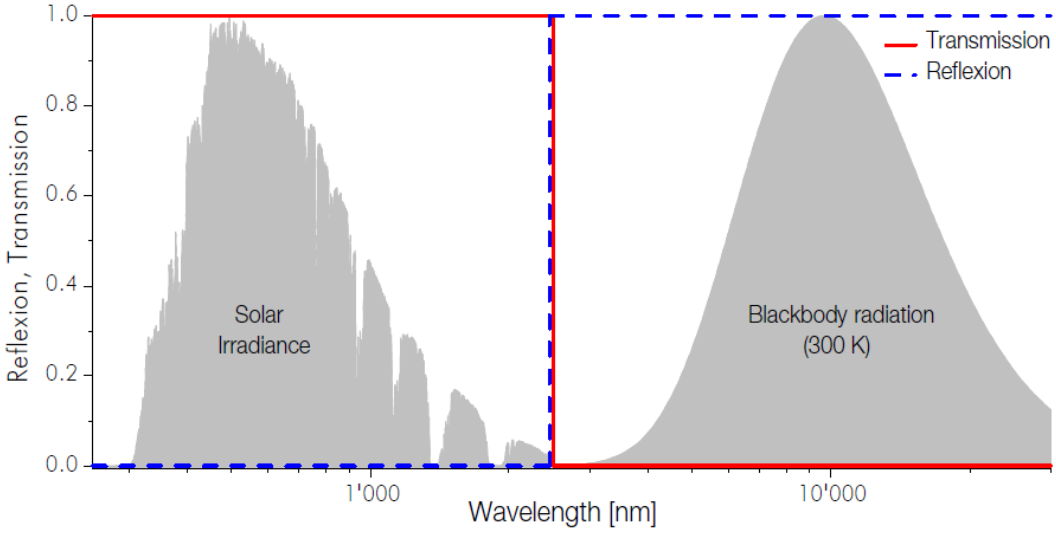

Figure 2 - Wavelength selectivity achieved by the nanomesh structure. Short-wavelength radiation are transmitted (a) and long-wavelength radiation are reflected (b).

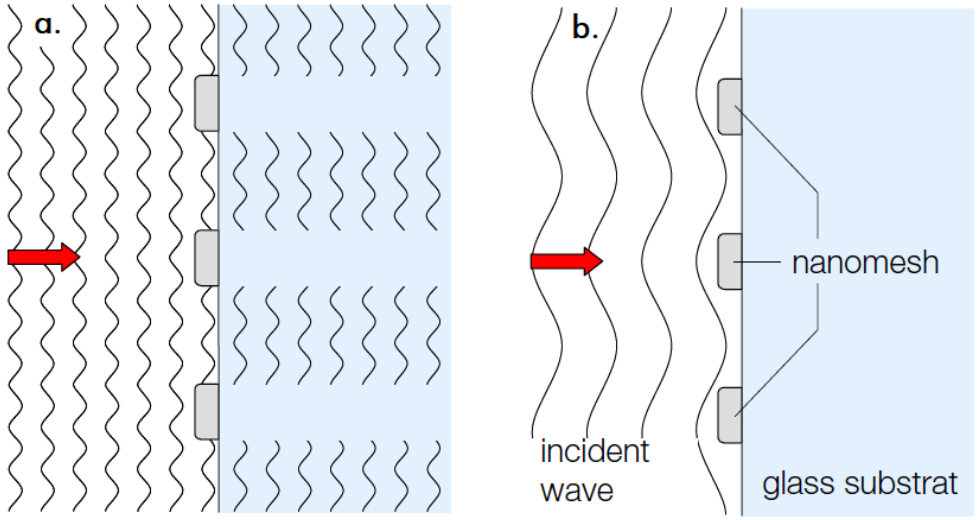

Figure 3 - Transmission and reflection spectra of an ideal solar gain coating. All the solar irradiance is transmitted to the building and the radiation from a blackbody at room temperature is reflected to keep the heat inside [5].

As simulated by M. Meier [5] in Figure 4, the selectivity of low-e coating after structuring is significantly improved. In the case of single glazing, 60 % of the loss in SHGC due the low-e coating can be regained by structuring the coating into nanomeshes. This number increases further to 80 % for double glazing. Another important aspect of the selectivity is the dimension of the structures. According to his simulation, the ideal grid periodicity should be of 1.875 μm with a linewidth of 1 μm and a thickness of 15 nm. This study presented promising results for future development of selective coating in buildings.

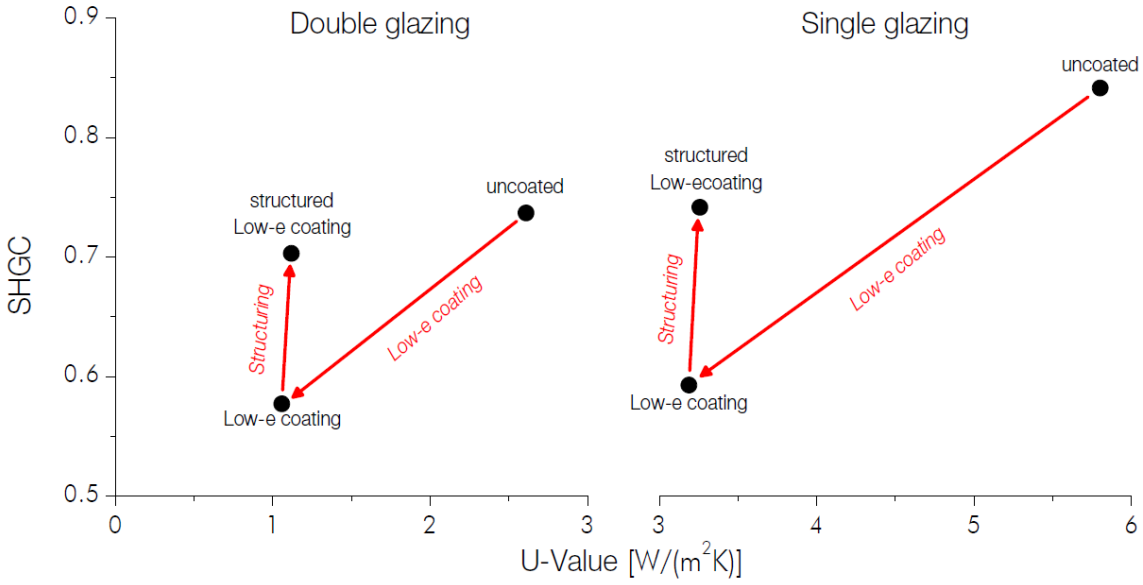

Figure 4 - Simulated values for single- and double-glazing application of structured coating. In that case, the creation of nanomeshes in the coating increases SHGC while limiting the loss in thermal insulation of the window.

Nowadays, the industry standard for energy efficient glazing consists of a triple glazing with two low-e coatings. According to the simulation tool provided by the glass company AGC [2], this type of windows achieves a U-value as low as 0.6 *W/(m²K)* but also comes with the drawback that only 55 % of solar heat gain is transmitted through the window. The implementation of nanomesh coating could potentially increase this value back to the original value of 73 % (without low-e coating). The calculated values found for a single, double, and triple glazing with or without low-e coating are showed in Table 1. It should be noted that these values do not match exactly with the ones found by Meier et al. This can be explained by the fact that characteristics of the glazing are not similar (air gap distance, type of glass, type of low-e coating, argon, or air in between the panes).

Table 1 - Optical properties of single, double, and triple glazing. For each glazing the panes consist of a clear-white 4 mm thick float glass and the air gap distance is always 14 mm filled with air or argon (Ar).

	Single Glazing		Double Glazing		Triple Glazing	
	n/a	Low-e	n/a	Low-e	n/a	Low-e
T_v	0.9	0.8	0.82	0.82	0.75	0.75
SHGC	0.88	0.71	0.8	0.63	0.73	0.55
U-Value (air)$[W/(m^2K)]$	5.8	3.5	2.8	1.5	1.8	0.8
U-Value (Ar) $[W/(m^2K)]$	n/a	n/a	2.6	1.2	1.7	0.6

Transparent conductive nanomesh coating

Electricity is conducted in the nanowires of the mesh. Therefore, a metallic nanomesh can be used as transparent electrode for switchable windows. Recently, Pil-Hoon Jung et al. reported a metal-nanomesh electrodes on flexible polymer film substrates. [6] Such transparent metal nanomesh electrodes are promising candidates to replace ITO. They achieve a high spectrally flat transmittance at wavelengths of 400 to 800 nm (above 80 %) and suitable electric properties (below 50 ohm/sq). The produced metal-nanomesh electrodes have suitable mechanical strength appropriate for flexible transparent electrodes. Figure 5 shows images of a metal-nanomesh on a polyethylene terephthalate (PET) substrate obtained by scanning electron microscopy (SEM) and photograph while the substrate was bent. High quality ITO films can be prepared with a sheet resistance in the same order of magnitude, but their spectral transmittance is not flat: they exhibit a cut-off wavelength early in the near infrared (NIR). Therefore, metal-nanomeshes have a superior potential especially for window applications where solar heat gains are desired. More considerations about ITO are listed in Table 2.

Table 2 - Advantages and disadvantages of ITO as transparent conductor.

Material	Advantages	Disadvantages
ITO	• High optical transparency (T = 85 - 95 %) • Low sheet resistance (Rs = 10 Ohm/sq) • Tunable work function (4.2 to 5.3 eV)	• Rare metal with rising cost • Limited supply and high demand • Brittle material (not suitable for flexible devices) • High temperature annealing • High refractive index • DC magnetron sputtering (vacuum)

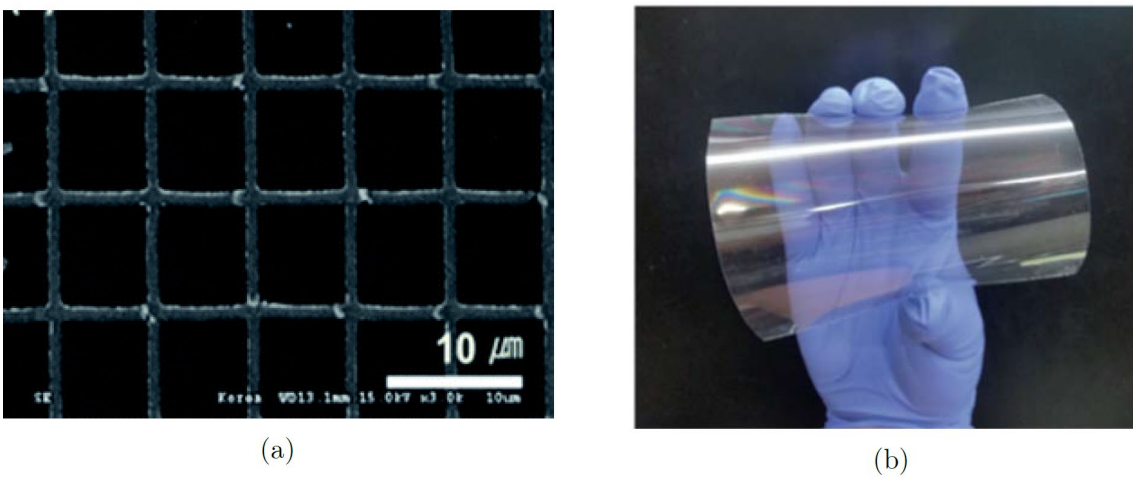

Figure 5 - (a) SEM image and (b) photograph of a flexible metal-nanomesh electrode on a PET substrate.

Highly conductive and transparent silver (Ag) honeycomb mesh have been fabricated by Kwon et al. using a monolayer of polystyrene spheres (see Figure 6, [7]). Ten-micron PS spheres were chosen as the template for the PS sphere monolayer, and heat pretreatment and Ag wet etching are used to demonstrate that the Ag honeycomb mesh electrodes have a high performance. The transmittance and the sheet resistance are, respectively, 83 % and 20 Ohm/sq, which are comparable to commercial ITO electrodes.

Table 3 exhibits a non-exhaustive list of additional publications comparing the optical and electrical properties of the obtained nanomesh structures. The first row gives the typical values found in the literature for the commercially available ITO, which provides transmittance of 85 to 95 % and sheet

resistance as low as 10 Ohm/*sq*. The best electrical performance was found by Gao at al. [8] with a sheet resistance of 0.7 Ohm/*sq*. To achieve such low resistance, they used a hierarchical multi-coating of metal nanomesh and microgrid. The structures consisted of a nanomesh of silver produced with the help of polystyrene spheres transfer. A honeycomb-microgrid was then added on top of it using photolithography. This process of hierarchical layers showed promising results.

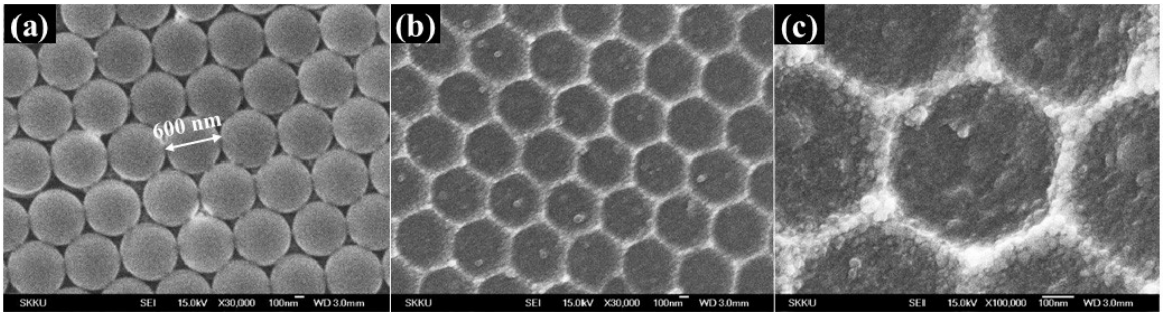

Figure 6 - FE-SEM images of (a) a 3 μm PS sphere monolayer and (b) Ag honeycomb mesh.
(c) Enlargement of the dotted box in (b)

Table 3 - Literature review about transparent conductor and their physical properties. Two important parameters: transmittance (at 550 nm) and sheet resistance are listed on the far right of the table.

Reference	**Transfer method**	**Material**	**Structure**	**Size**	**Thickness**	**Trans.[%]** (550 nm)	**Sheet res.** [Ohm/*sq*]
Sigma Aldrich	Sputtering	ITO	Coating	n/a	15-100 nm	85-95	10-90
Kwon2013 [7]	PS- Spheres	Ag	Honeycomb	0.6, 3, 10 um	300 nm	83	20
Ho2011 [9]	PS-Spheres	Ag	Honeycomb	0.6 um	20 nm	85	35
Ho2013 [10]	PS-Spheres	Ag	Honeycomb	0.6 um	15 nm	74.2	30
Gao2015 [8]	PS-Spheres/ photolithography	Ag	Hole/ Honeycomb	2um/ 500 um	30 nm/ 1 um	83	0.7
Kim2015 [11]	Photolithography	Cu+ZnO:Al	Honeycomb	5-30 um	62 nm	90.6	6.2
Jung2016 [6]	Embossing	Cu/Au	Grid pattern	500 nm / 7 um	50/100 nm	80	50
Choi2015 [12]	Embossing	Ag	Grid pattern	7.5, 10 um	100 nm	85	10
Oh2012 [13]	Embossing	Ag	Grid pattern	200 nm	n/a	28	23
Jang2013 [14]	AAO template	Pt	Honeycomb	22 nm	30 nm	75.2	71
Paeng2015 [15]	Laser ablation	Cu	Honeycomb	4.7 um	19 nm	83	17.5

WP1 highlights:
A literature review indicates promising potential for selective low-e coating in cool climate and brings forward the need for more effective transparent conductive coating, especially for electrochromic devices. Various suggestions of principle how to produce nanomesh in a scale have been proposed. Few information was found about hybrid structure with high transmittance and low sheet resistance.

WP2: Design of nanomeshes based on a theoretical understanding of the underlying principles

The first step to understand the interaction between light and the nanomeshes consisted in simulating the EM-waves using Maxwell's equations and a finite-difference time-domain (FDTD) solver called "Lumerical". This type of simulation predicts the specific frequencies that might interact with the nanomesh structure and provide valuable information about adequate nanomesh-scale that will act to our advantage. A specially designed High-Performance Computer (HPC) was built for this type of simulation. It consists of a server with 32 cores (2 x 16 processors) with a total of 256 GB of fast RAM and a professional high-end graphic card (NVIDIA Quadro RTX 5000) allowing for GPU-enhanced calculation. This setup provides a state-of-the-art HPC for complex 3D simulation and fast optimization of multiples parameters.

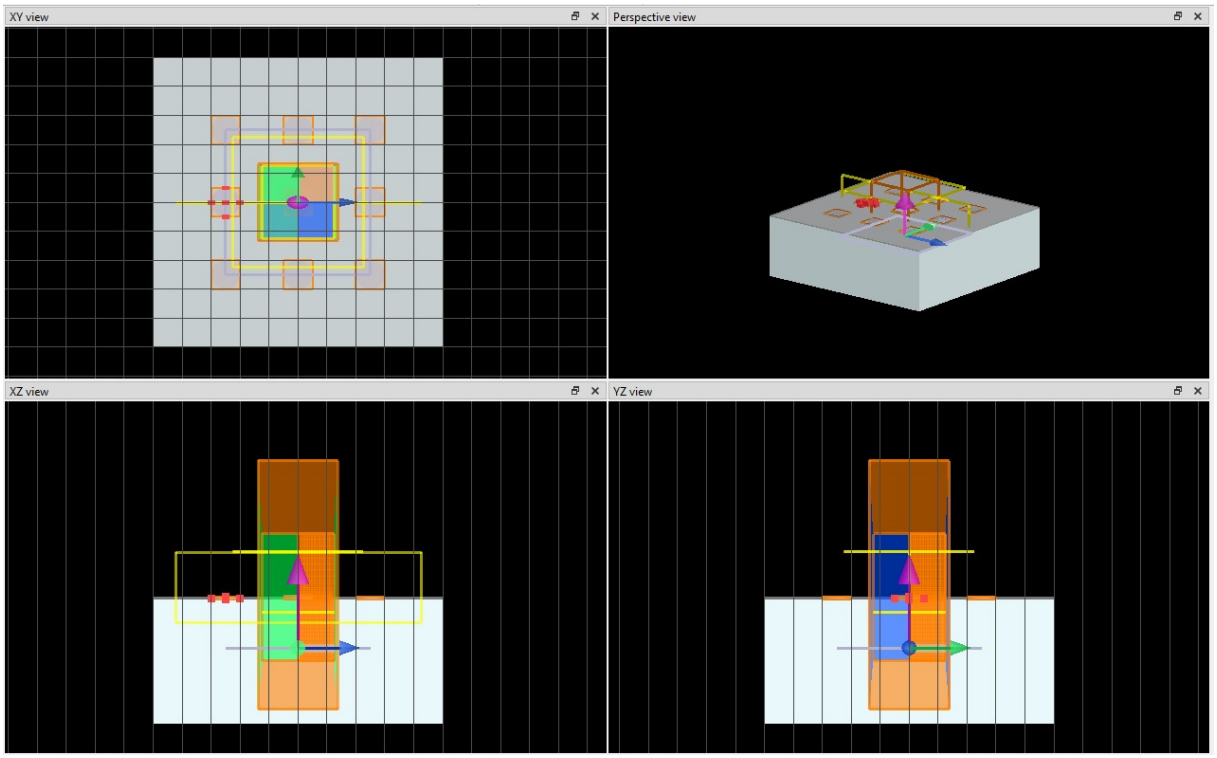

Figure 7 – Layout Lumerical Software where the large white rectangle represents a glass substrate of 4x4 um covered by a silver coating of 50 nm. In this case, the nanomesh consist of holes with a diameter of 400 nm. The orange rectangle describes the FDTD simulation region where the purple arrow is the incoming EM-wave and each lateral side have periodic boundary conditions.

The first simulations were done using the FDTD method for modelling the light/matter interaction of an incoming beam on a nanomesh structure as shown in Figure 7. To confirm the validity of our software, various structures were taken from the literature [5], [16] and replicated. The results are presented in Figure 9 and Figure 8. These findings confirmed the accuracy of the software which was also used in WP6 for the enhancement in selectivity of low-e coatings.

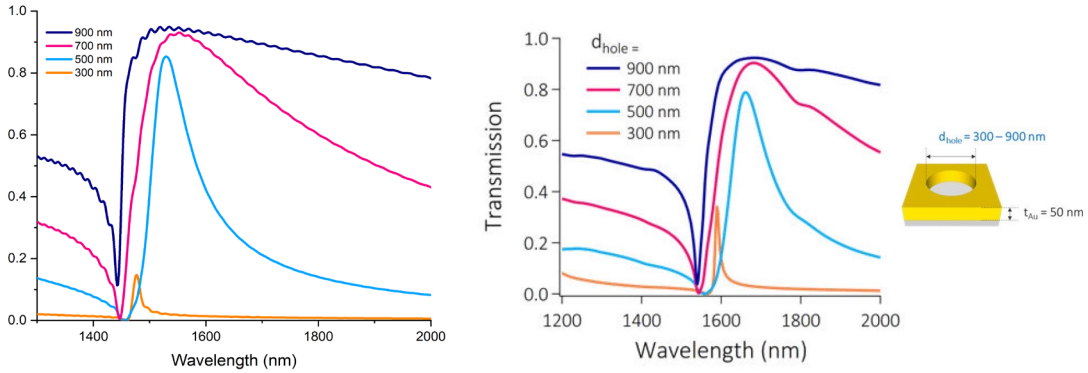

Figure 8 - Simulated transmission spectra of Au nano-holes array as a function of nano-hole diameter. Where a) describes our results and b) the results based on simulation done by Q. Tong et al. [16] The minima and maxima of each curves is slightly shifted to the left in our simulation. This can be explained by the fact that different n and k value for the materials has been used, but the general behavior is similar.

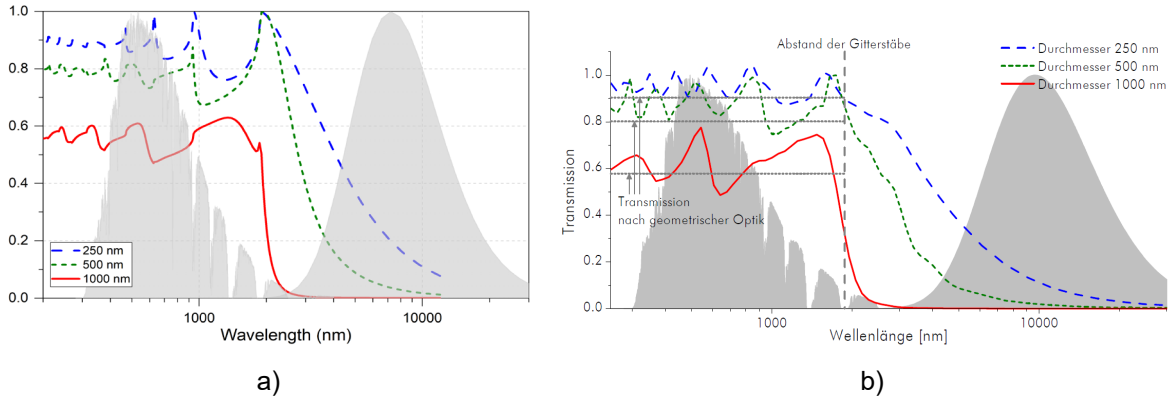

Figure 9 - Spectral transmission of an incoming light wave at normal angle through a mesh of metallic rods. The grey areas represent on the left, the solar radiation and on the right, the black body radiation at 300 K. The rods are spaced with a periodicity of 1875 nm and their diameter is varied between 250, 500, 1000 nm. Where a) describes our results and b) the results based on simulation done by M. Meier [5]. The slight difference in the curves can be explained by the periodic boundary conditions used in our simulation which was not implemented in the case of Meier's calculation.

More simulation on periodic structures can be found in the confidential section.

Furthermore, a design for electrical conducive nanomesh was investigated and is presented in Figure 10. A boundary condition of maximum 4 % surface coverage $(w/p)^2$ was chosen for high light transmittance. A design is proposed in the confidential report and is achieving a theoretical sheet resistance of 1.6 Ohm/sq based on a silver mesh leading to sheet resistance much lower than the best available ITO coatings on the market.

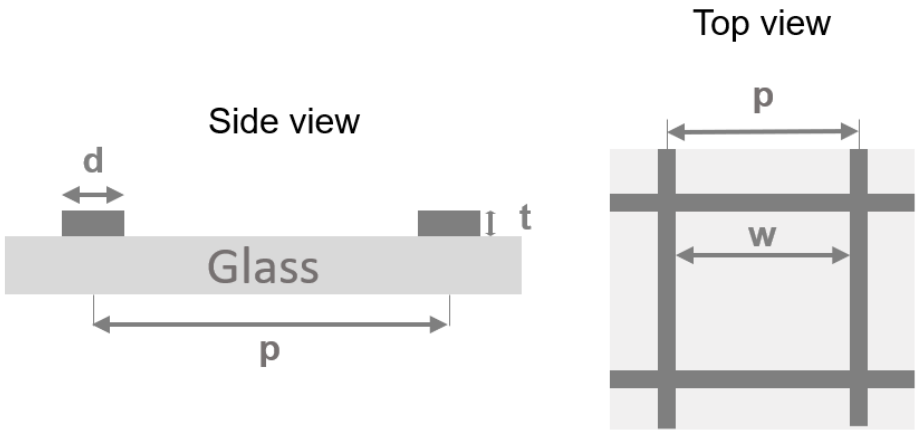

Figure 10 - Schematic drawing of top view of a metallic nanomesh with “d” being the width of each line, “t” the thickness, “p” the periodicity of the unit cell and “w” the size of the opening.

WP2 highlights:

FDTD simulations were performed on a specially designed High-Performance Computer. Lumerical software was used to, first, validate the accuracy of our model based on the literature and then, various parameters were optimized.

In a second part, a nanomesh structure was design based on theoretical electrical and optical properties.

WP3: Origination of micro-/nano- structures

WP3.1 Transparent conductive micro/nanomesh coating by laser ablation structuring

Following the literature research presented above, the first attempt in structuration of a metallic coating was performed using the equipment already available in our lab. As presented by Paeang et al. [15], laser ablation method gave promising electrical and optical properties (Transmittance: 83 %, Sheet resistance: 17.5 Ohm/sq). Figure 11 illustrates the structure chosen for this experiment which consists of a multilayer of thin films deposited by reactive magnetron plasma sputtering: first a titanium seed layer was deposited on a glass substrate to increase the adhesion at the interface. Then 10 and 20 nm of copper was added and passivated with 1 nm of titanium at the top.

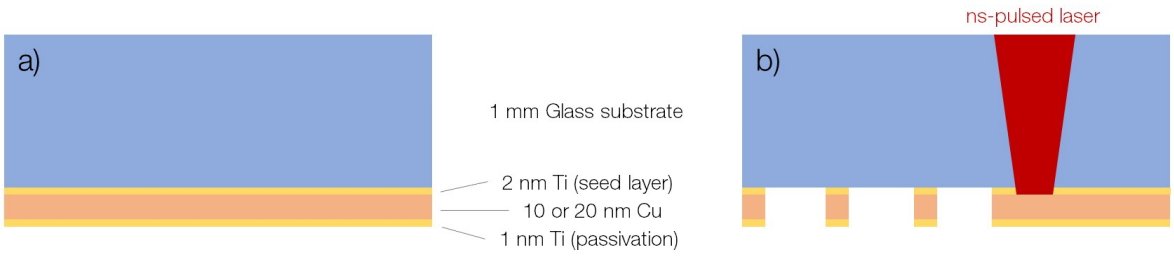

Figure 11 - Multiple layers stack consisting of a glass substrate, titanium seed layer, copper as conductor and another titanium layer as a passivation protection coating. (a) as-deposited sample (b) after laser-structuring.

As shown in Figure 11b, a laser ablation of the coating was done using a 1064-nm nanosecond fiber laser with a FWHM pulse duration of 30 ns. The resulted patterns are shown in Figure 12. The size of each hole is approx. 20 µm in diameter and the distance between each circle is 35 µm.

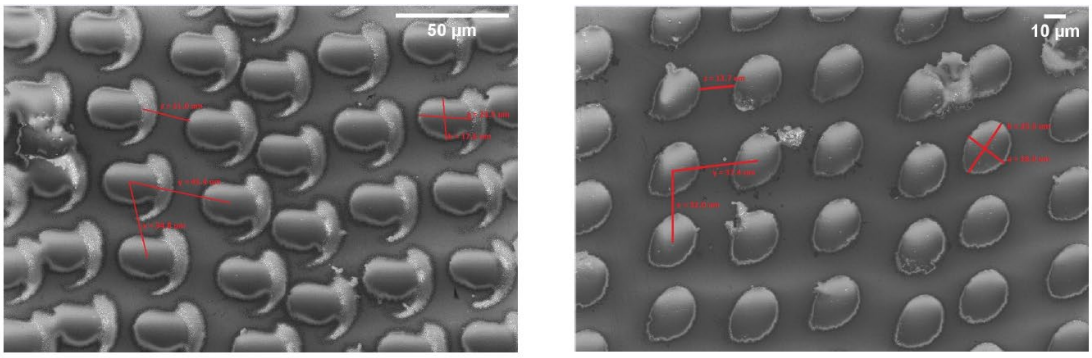

Figure 12 - SEM-image of laser-ablated pattern obtained for a thickness of (a) 10 nm and (b) 20 nm.

The transmittance at 550 nm of the fabricated samples were measured using an integrating sphere combined with a UV/VIS spectrophotometer. Four-point probe Van der Pauw method was then used to measure the sheet resistance. The corresponding values are showed in Table 4. For both samples, the increase in transmittance after structuring was significant: 16 % and 23 % gain for, respectively, 10 and 20 nm Cu thicknesses. The improvement in transparency can also clearly be seen in the photos presented in Figure 13. In the case of the thin sample (10 nm), the sheet resistance showed a surprising 17-fold increase. This can be explained by the fact that, for this sample, the ablation resulted in additional removal of the coating (see Figure 12a). It is thought that laser beam was not focused exactly on the coating, which led to a non-uniform ablation and thus, higher sheet resistance. The laser ablation for the sample with a thickness of 20 nm was more precise and led to minor decrease in electrical performance.

Table 4 - Optical and electrical properties of as-deposited and laser-patterned copper samples.

	Transmittance (at 550 nm) [%]		Sheet Resistance [Ω/sq]	
Cu-Thickness	As-deposited	Laser-patterned	As-deposited	Laser-patterned
10 nm	45	61	5.8	101.0
20 nm	25	48	1.8	7.4

These results showed that copper could be a promising candidate for an application in electrochromic windows, where good transmittance and conductivity are essential. The film thickness still needs to be optimized to maintain a balance between the sheet resistance and visible transmittance. The laser process was done as a post treatment and could easily be applied at the back end of a glass production line.

Figure 13 - Photos of Copper thin film samples non-ablated (left) and laser patterned (right) with a thickness of (a) 10 nm and (b) 20 nm.

WP3.2 Transparent conductive micro/nanomesh coating by photolithography

The origination of micro-/nano- structure by photolithography was investigated in the Center of Micro/Nanotechnology CMI at EPFL. To access the facility, an extensive safety course and a training on each machine had to be followed. The goal of this work package was to produce samples with high transparency and good conductivity that could then be used as a transparent electrode in an electrochromic device. The chosen design was presented in Figure 10 and the process outline used to produce this nanomesh structures is shown in Figure 14.

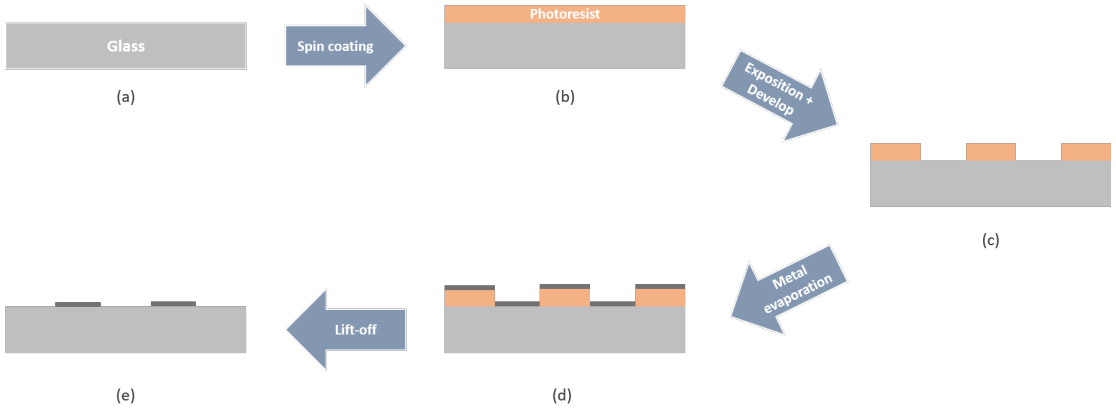

Figure 14 - Step-by-step process outline of the production of silver nanomeshes using UV-photolithography. The substrate (a), consisting of soda-lime glass, is spin-coated with a negative photoresist (b). The sample is locally exposed to a UV-laser to harden the photoresist and is followed by the development which removes the non-exposed resist (c). A thin metallic film is then evaporated over the sample (d) and, finally, the remaining photoresist is lifted-off in a chemical bath resulting in the nanomesh structure (e).

As it can be seen in Figure 15, the SEM image shows a well-defined structure and sharp edges. As a first step, this pattern could not be achieved over the entire area of a 10 cm wafer due to a weak adhesion between glass and silver (see Figure 16). To fix this issue, a new adhesion layer of 10 nm titanium was added to the sample which resolved the delamination of the silver film.

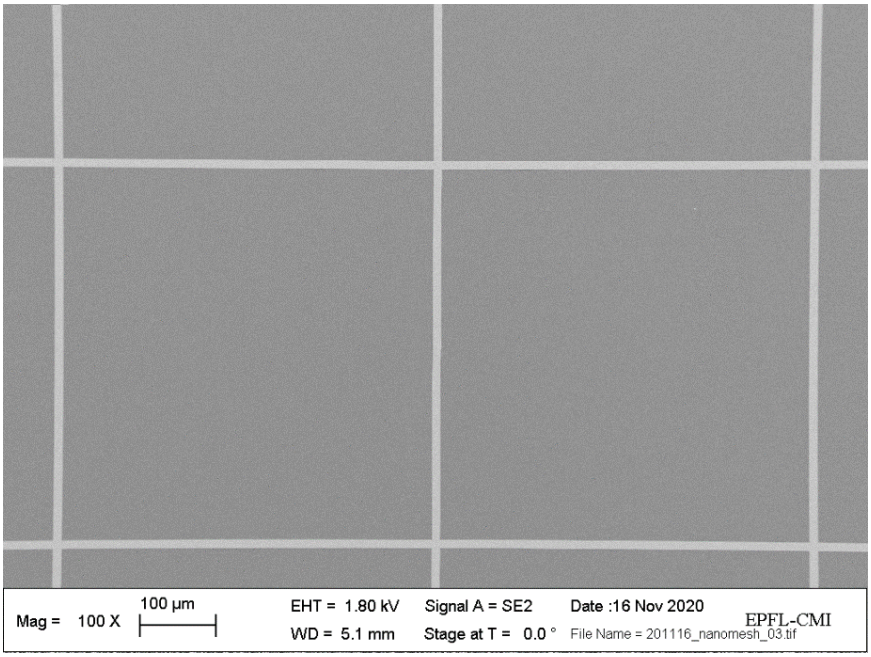

Figure 15 - SEM image of nanomesh produced at CMi with a periodicity (p) of 500 um, a line width (d) of 10 um and a thickness (t) of 200 nm.

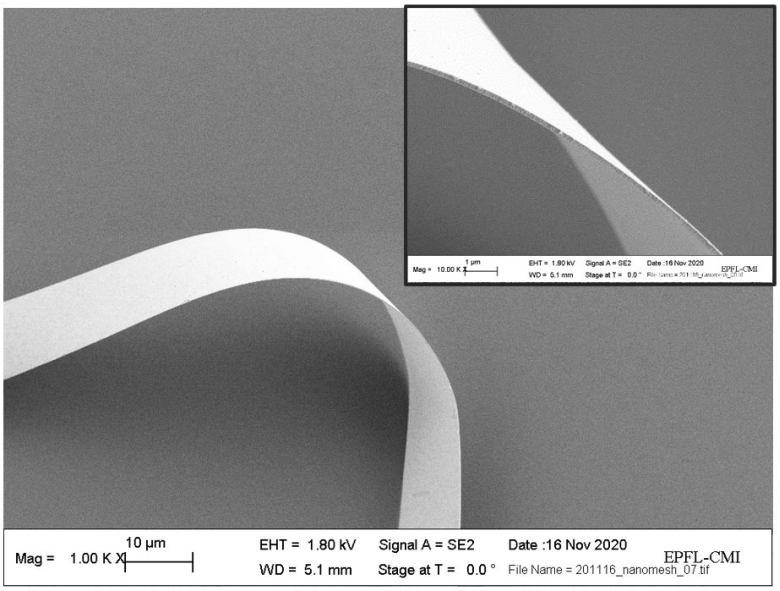

Figure 16 - SEM image of silver nanomesh produced at CMi. This specific segment was delaminated during the lift off process because of poor adhesion to the glass substrate. The inset image shows a close-up view of the bended 200 nm thick silver film.

WP3 highlights:

Laser ablation processing can produce micromeshes, enhancing the visible and solar energy transmittance (Tv and Te). The treatment happens after the deposition of the coating (back end) which represents a logistical advantage for large scale production. Well-defined structures in the 1 to 10 um range can be made using UV-photolithography. This process results in high resolution and reproducible micromeshes but requests more infrastructures.

WP4: Replication of micro-/nano- structures

As presented in WP3.1, laser structuring of conductive micro/nanomesh coating is a promising process for origination purposes. This approach could also be used to replicate micro-/nano- structures in a large scale as presented in our previous works [17], [18]. A market study has been carried out on UV-picosecond laser in the preparation of the upcoming purchase of a new laser.

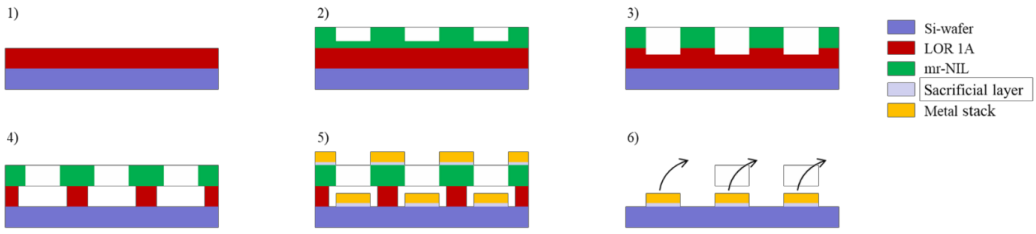

Figure 17 - Schematics of our nanoimprint fabrication process. A wafer is spin-coated with a photoresist (LOR1A) (1) and imprinted using mr-NIL212FC_XP with a soft h-PDMS/PDMS stamp (2). After oxygen plasma etching (3) and wet chemical etching (4), the desired layer stack is deposited (5). Through immersion in MF24 A the mask is lifted-off (6) and the nanoparticles are ready for particle lift-off via wet-chemical etching of the sacrificial layer [19].

On the topic of nanoimprint lithography, a collaboration with Tina Mitteramskogler from the company PROFACTOR in Austria led to promising results. The nanoimprint process used for the replication of the nanostructured is presented as a schematic in Figure 17.

The SEM images of the resulting samples are shown in Figure 18. The diameter of each hole is 1.9 um and the periodicity 3 um.

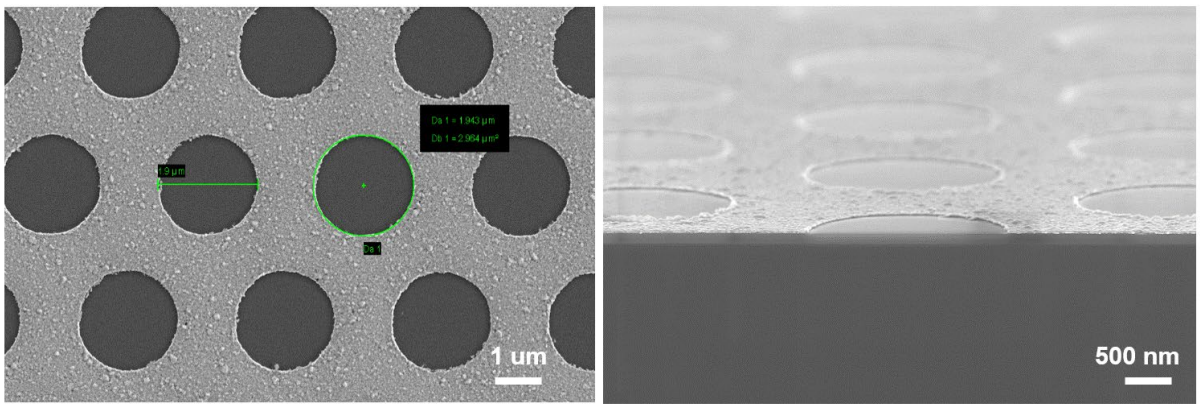

a) b)

Figure 18 - SEM images showing the resulting wafer achieved by nanoimprint lithography. The diameter of each hole is approx. 1.9 um, the periodicity 3 um and the thickness of the silver layer 20 nm. a) top-down view of the structures and b) 10.5° tilted of a cross-section.

WP4 highlights:

Nanoimprint lithography represents a powerful process and allow the reproduction of well-defined, nanoscale structures. It consists of a front-end treatment (before coating) which could make it more challenging to apply for industrial production.

WP5: Characterization of nanomeshes (SEM, UV-VIS-NIR spectrophotometry, FTIR spectrophotometry in the MIR, electrical conductivity)

The results from the methods used for the characterization of the sample are presented directly in the results section. It consists, as shown in Figure 19 of Scanning Electron Microscope (SEM) images taken on a Gemini 300 from ZEISS, transmission spectra measured with a UV-VIS-NIR spectrophotometer, MIR emissivity with a FTIR spectrophotometry and electrical conductivity measured with a Four-point-probe setup that allowed us to determine the sheet resistance of our metal nanomeshes, and to compare them to conventional TCO films.

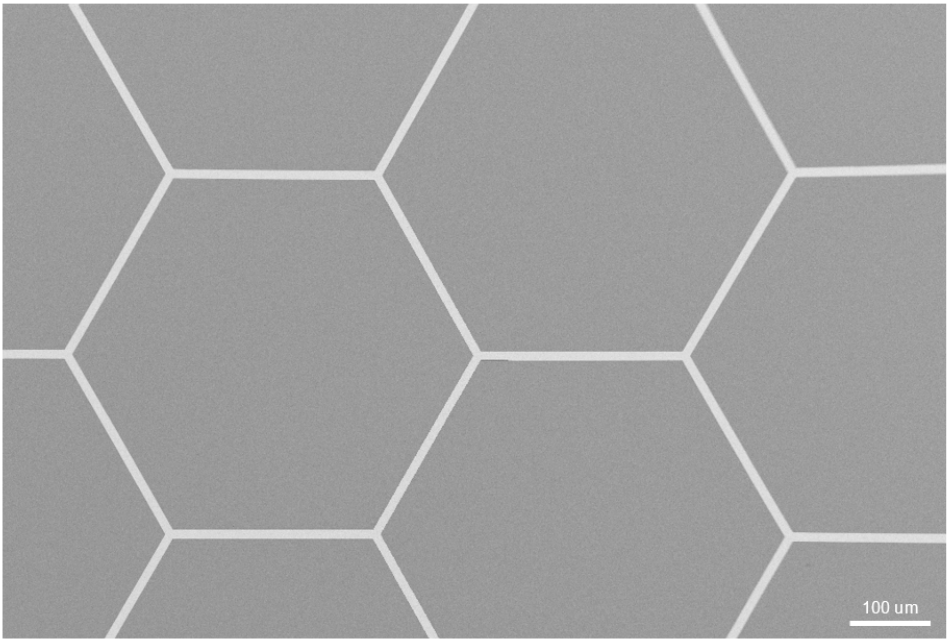

Figure 19 - Honeycomb-structured micromesh taken with a scanning electron microscope

WP5 highlights: SEM is a useful tool to characterize micro and nanoscale structure and was widely used during this project to analyse the quality of the nanomeshes. Optical and electrical measurements were also crucial for the characterization of the transparent conductors.

WP6: Enhancing the selectivity of a low-e coating

FDTD method presented in WP2 is used in this section to deepen the understanding of selective low-e coatings and predict the correct dimension for optimized results. As shown in Figure 20, the size and periodicity of the mesh are crucial parameters to define the selectivity of the structure. In this case, on one hand the visible light (550 nm) is transmitted through the mesh whereas, on the other hand, mid-infrared radiations (15 um) are entirely reflected, thus acting as a heat-mirror.

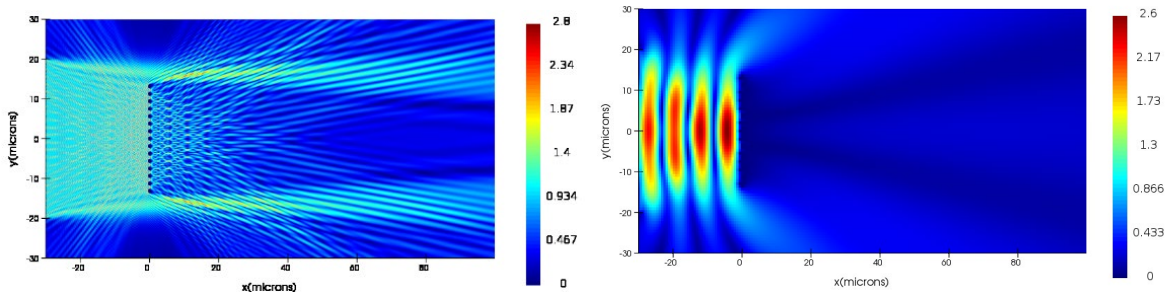

a) b)

Figure 20 - FDTD simulations of electromagnetic wave transmission through a metallic mesh with a periodicity of 1'875 nm and mesh openings of 875 nm. The colors indicate the relative intensity of the electrical component for an electromagnetic wave with a wavelength of a) 550 nm which is partially transmitted through the mesh and b) 15 um (entirely reflected). Polarization is perpendicular to the plane of observation.

Figure 21 presents a photograph of the samples produced in WP 4 and shows a significant increase in optical transmission between the treated and non-treated sample. The VIS and NIR transmission was measured with the spectrometer and is illustrated in Figure 22. As shown in Table 5, the transmittance of the nanoimprint sample was increased by up to 25 % in the visible and near infrared spectrum. More results about the mid infrared reflectance are presented in the confidential report.

Figure 21 - Photograph of the 20 nm silver coating (on the left) compared to the nanoimprint-structured sample (on the right).

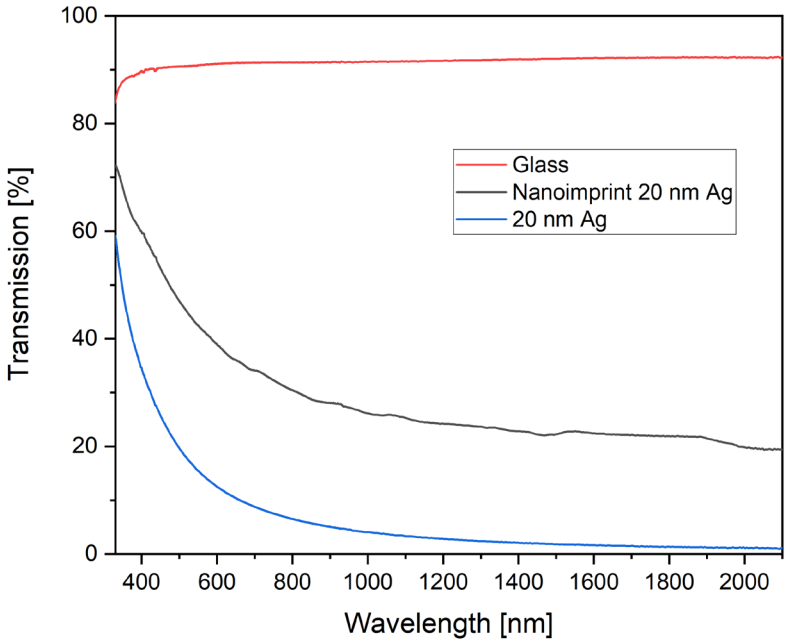

Figure 22 - Transmission spectra comparing a simple glass slide without any coating, with a 20 nm Silver thin film and a structured coating. The nanoimprint process increased the transmittance by 20 – 25 % over the measured range.

Table 5 - Visible and solar energy transmittance (T_v and T_e) and reflectance of 20 nm silver coating with and without nanoimprint lithography.

Sample	T_e[%]	T_v [%]	Reflectance [%]
20 nm Ag	11.9	14.4	97
Nanoimprint 20 nm Ag	34.2	39.3	72

WP6 highlights:

The spectral selectivity of a periodic structure was simulated with the FDTD method and showed a high transmittance for EM-waves in the visible spectrum as well as high reflectance in the far infrared. This result was tested on a sample produced by nanoimprint lithography and showed promising results.

WP7: Study of hybrid structures with metal nanomeshes and thin TCO layers

On the topic of TCO layers, commercially available ITO coatings were analyzed, and the properties of ultra-transparent thin ITO film were identified. These specific coatings could potentially be well suited for application in hybrid structure, combining ITO and metal nanomeshes for increased electrical performance.

The results of this section are presented in the confidential report

WP7 highlights:

Hybrid nanomeshes were produced, exhibiting higher visible transmittance and lower sheet resistance which are the two most important parameters for electrochromic devices. Moreover, nanomeshes allow for a large spectral range transmittance in the near infrared which improves the solar heat gain during the cold months.

WP8: Preparation of electrochromic device with metal nanomeshes as a conductive transparent layer

The first attempt in creating an electrochromic device was done using a silver micromesh with a periodicity of 500 um and linewidth of 10 um as conductive transparent layer. A 1'000 nm thick coating of $MoWO_3$ was selected as electrochromic material for its large spectral range, color neutral and fast switching properties.[20] The resulting coloration can be seen in Figure 23. This first attempt brought out some interesting facts about this configuration:

- The coloration happens in the entire surface of the coating, meaning that the micromesh fulfils its purpose as a conductive layer.
- The yellowing effect around the silver conductor is due to corrosion of the metal by the liquid electrolyte used in this experiment which leads to the degradation of the mesh.

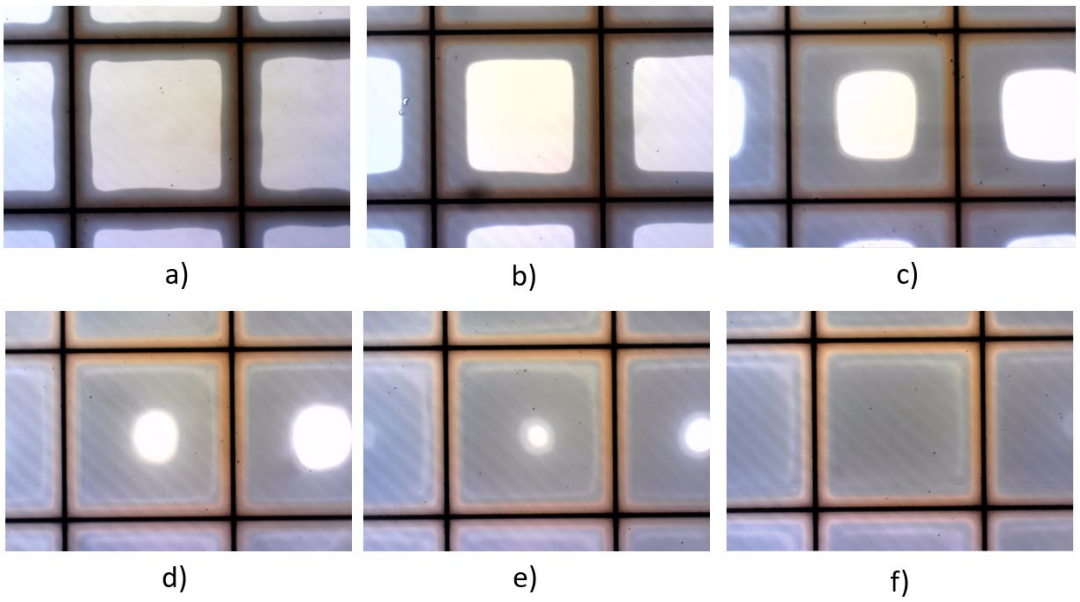

Figure 23 - Coloration of electrochromic coating based on 10 um thick silver micromeshes where the color changes, a) starting from the conductive mesh and f) spreading to the center of the unit cell.

To resolve this drawback, platinum micromesh was used for the second attempt and showed promising results. The final configuration of the micromesh consisted of a 10 nm titanium adhesion layer followed by a 200 nm platinum coating which was not impacted by the electrolyte during coloration. The resulting sample is shown in a SEM image in Figure 24 and in a photograph in Figure 25. At this scale (2 um), the micromeshes are invisible to the naked eyes and exhibit high transmittance.

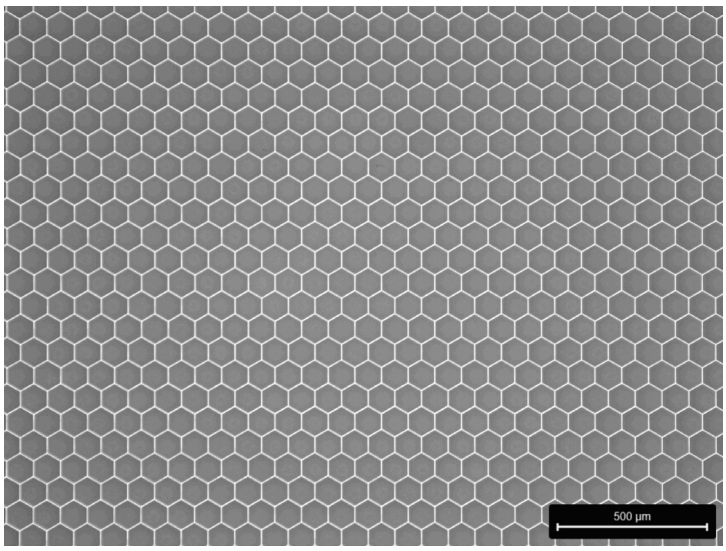

Figure 24 – SEM image of a honeycomb-structured micromesh with a linewidth of 2 um and a periodicity of 100 um

Figure 25 – Left: reference float glass and right: honeycomb micromesh with a linewidth of 2 um

Finally, a full electrochromic device was built based on nanomeshes as transparent conductors, $MoWO_3$ as electrochromic electrode and NiTaO as counter-electrode (see Figure 26). This first device was switching in a matter of 1 or 2 seconds and exhibits a large spectral range in the near infrared which represents promising results for future applications in electrochromic windows.

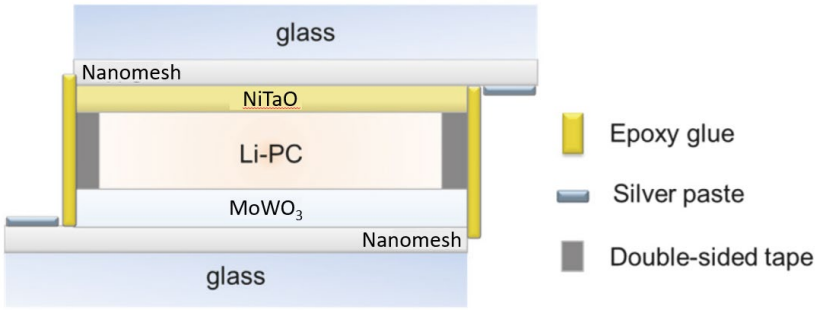

Figure 26 - Electrochromic device with a liquid electrolyte placed between two nanomesh glass coated with an anodic and cathodic electrochromic oxide.

WP8 highlights:

A full electrochromic device based on nanomeshes was fabricated on a lab scale and exhibited a large spectral range, fast and color neutral switching.

WP9: Evaluation of feasibility of envisaged applications (insulating glazing with enhanced selectivity, electrochromic windows)

The proof of concept of insulating glazing with enhanced selectivity was shown in WP 6 and the envisaged applications could consist of residential buildings with low windows to wall ratio or box type solar cooker. This technology gives the significant advantage to increase the solar heat gain while maintaining excellent insulation properties.

The fabrication of a full electrochromic device in WP 8 showed that nanomeshes are well suited for this type of application and offer a large spectral range, fast and color neutral switching. The challenges for a market implementation faced by both applications are the production process which has to be done either before (front-end treatment based on lithography) or after (back-end laser ablation) the deposition of the coating.

4 Conclusions

The literature review indicates promising potential for selective low-e coating in cool climate and brings forward the need for more effective transparent conductive coating, especially for electrochromic devices. Various theoretical principles on how to produce nanomesh in a scale have been proposed.

FDTD simulations were performed on a specially designed High-Performance Computer. Lumerical software was used to, first, validate the accuracy of our model based on the literature and then, various parameters were optimized. Additionally, a nanomesh structure was design based on theoretical electrical and optical characteristics.

Laser ablation processing can produce micromeshes, enhancing the visible and solar energy transmittance (Tv and Te). The treatment happens after the deposition of the coating (back end) which represents a logistical advantage for large scale production. Well-defined structures in the 1 to 10 um range can be made using UV-photolithography. This process results in high resolution and reproducible micromeshes but requests more infrastructures.

Nanoimprint lithography represents a powerful process and allow the reproduction of well-defined, nanoscale structures. It consists of a front-end treatment (before coating) which could make it more challenging to apply for industrial production.

SEM is a useful tool to characterize micro and nanoscale structure and was widely used during this project to analyze the quality of the nanomeshes. Optical and electrical measurements were also crucial for the characterization of the transparent conductors.

The spectral selectivity of a periodic structure was simulated with the FDTD method and showed a high transmittance for EM-waves in the visible spectrum as well as high reflectance in the far infrared. This result was tested on a sample produced by nanoimprint lithography and showed promising results.

Hybrid nanomeshes were produced, exhibiting higher visible transmittance and lower sheet resistance which are the two most important parameters for electrochromic devices. Moreover, nanomeshes allow for a large spectral range transmittance in the near infrared which improves the solar heat gain during the cold months.

A full electrochromic device based on nanomeshes was fabricated on a lab scale and exhibited a large spectral range, fast and color neutral switching.

5 Outlook and next steps

Future work on this topic could include two directions:

The implementation of hybrid nanomeshes in electrochromic devices for large spectral range, color neutral and fast switching. More work needs to be carried out regarding the electrochromic materials used in this type of device and their combination with transparent conductors.

Large scale fabrication of nanomeshes with spectral selectivity for high solar heat gain and excellent thermal insulation. This type of coatings could be used on the windows in colder climate or on the glass of a solar box cooker.

6 National and international cooperation

- Active scientific collaboration with Dr. Matthias Krause (Head Nanocomposite Materials) and visit of the Helmholtz-Zentrum in Dresden-Rossendorf.
- Scientific interaction and discussion with prof. Ramon Escobar Galindo at the Applied Physics I department “Research on new materials for energy and biomedical applications” at the university of Sevilla.
- Collaboration and scientific discussion about simulation software “HFSS” with Mauro Di Domenico at SUPSI in Lugano.
- Close contact with researchers from SCCER FEEB&D on the project about electrochromic windows and glazing with microstructures.
- Within EPFL, access to electron microscopes and to the facilities of SEM imaging provided by the Interdepartmental Center of Electron Microscopy CIME and clean room environment for Photolithography at the Center of Micro / Nanotechnology CMI.
- Active collaboration on X-ray diffraction analysis related matters with Dr. Arnaud Magrez, head of the Crystal Growth Facility at EPFL.

- Collaboration and scientific discussion about simulation software “Lumerical” with Prof. Anna Fontcuberta and her research group at EPFL.
- Discussion about large area origination by laser ablation have been conducted with Prof. Patrik Hoffmann at EMPA Thun.
- SCALAR Project, EMPA, 3D AG
- Collaboration with the startup Infrascreen about Greenhouse insolation
- Discussions about nanomeshes with CSEM and Mecaplex

7 Industry contacts

- Partnership with SWISSINSO: Technology transfer of magnetron sputtering and research on novel coatings for innovative solar glazing.
- Interaction and discussion with Dr. Jörg Neidhart (Head of innovation and technology application) at VON ARDENNE: manufacturer of advanced coating equipment.
- Scientific publication and patent on smart windows with Nima Jamaly and Stefan Mauron from Swisscom.
- Partnership with the Bern-Lötschberg-Simplon-Bahn train company and the glass company AGC: Technology transfer of laser structured efficient windows.
- Collaboration with Tina Mitteramskogler from the company PROFACTOR in Austria on samples for nanoimprint transfer technology.
- First contact with Flachglas has been established about MIMO friendly windows.

8 Publications

In the field of structured low-e coating, 2 publications were/are going to be published:

- Fleury, Jeremy, et al. "Wide band-pass FSS with reduced periodicity for energy efficient windows at higher frequencies." *Applied Physics A* 126 (2020): 417.
- Manuscript in preparation: L. Burnier, N. Jamaly, J. Fleury, and A. Schüler, “Energy saving glazing with high MIMO performance.”

9 References

[1] A. Kemmler, “Analyse des schweizerischen Energieverbrauchs 2000-2017.” Bundesamt für Energie, Bern, 2018.
[2] AGC, “Glass Configurator AGC Glass Europe.” https://www.agcyourglass.com/configurator/en. Accessed: 26-09-2019.

[3] M. Lokanc, R. Eggert, and M. Redlinger, “The Availability of Indium: The Present, Medium Term, and Long Term,” NREL/SR--6A20-62409, 1327212, Oct. 2015. Accessed: Jun. 18, 2019. [Online]. Available: http://www.osti.gov/servlets/purl/1327212/
[4] S. D. Rezaei, S. Shannigrahi, and S. Ramakrishna, “A review of conventional, advanced, and smart glazing technologies and materials for improving indoor environment,” *Sol. Energy Mater. Sol. Cells*, vol. 159, pp. 26–51, Jan. 2017, doi: 10.1016/j.solmat.2016.08.026.
[5] M. Meier, “Mikrostukturierte Metallschichten auf Glas,” Bayerischen Julius-Maximilians-Universität Würzburg, 2006.
[6] P.-H. Jung, Y. Doo Kim, H.-J. Choi, Y. Hoon Sung, and H. Lee, “A transparent embedded Cu/Au-nanomesh electrode on flexible polymer film substrates,” *RSC Adv.*, vol. 6, no. 95, pp. 92970–92974, 2016, doi: 10.1039/C6RA12054G.
[7] N. Kwon, K. Kim, S. Sung, I. Yi, and I. Chung, “Highly conductive and transparent Ag honeycomb mesh fabricated using a monolayer of polystyrene spheres,” *Nanotechnology*, vol. 24, no. 23, p. 235205, 2013, doi: 10.1088/0957-4484/24/23/235205.
[8] T. Gao, P.-S. Huang, J.-K. Lee, and P. W. Leu, “Hierarchical metal nanomesh/microgrid structures for high performance transparent electrodes,” *RSC Adv.*, vol. 5, no. 87, pp. 70713–70717, Aug. 2015, doi: 10.1039/C5RA14851K.
[9] Y.-H. Ho, K.-Y. Chen, S.-W. Liu, Y.-T. Chang, D.-W. Huang, and P.-K. Wei, “Transparent and conductive metallic electrodes fabricated by using nanosphere lithography,” *Org. Electron.*, vol. 12, no. 6, pp. 961–965, Jun. 2011, doi: 10.1016/j.orgel.2011.03.019.
[10] Y.-H. Ho, K.-Y. Chen, K.-Y. Peng, M.-C. Tsai, W.-C. Tian, and P.-K. Wei, “Enhanced light out-coupling of organic light-emitting diode using metallic nanomesh electrodes and microlens array,” *Opt. Express*, vol. 21, no. 7, pp. 8535–8543, Apr. 2013, doi: 10.1364/OE.21.008535.
[11] W.-K. Kim *et al.*, “Cu Mesh for Flexible Transparent Conductive Electrodes,” *Sci. Rep.*, vol. 5, p. 10715, Jun. 2015, doi: 10.1038/srep10715.
[12] H.-J. Choi, S. Choo, P.-H. Jung, J.-H. Shin, Y.-D. Kim, and H. Lee, “Uniformly embedded silver nanomesh as highly bendable transparent conducting electrode,” *Nanotechnology*, vol. 26, no. 5, p. 055305, 2015, doi: 10.1088/0957-4484/26/5/055305.
[13] S.-C. Oh *et al.*, “Various metallic nano-sized patterns fabricated using an Ag ink printing technique,” *Electron. Mater. Lett.*, vol. 8, no. 5, pp. 485–489, Oct. 2012, doi: 10.1007/s13391-012-2053-7.
[14] H. Y. Jang, S.-K. Lee, S. H. Cho, J.-H. Ahn, and S. Park, “Fabrication of Metallic Nanomesh: Pt Nano-Mesh as a Proof of Concept for Stretchable and Transparent Electrodes,” *Chem. Mater.*, vol. 25, no. 17, pp. 3535–3538, Sep. 2013, doi: 10.1021/cm402085k.
[15] D. Paeng *et al.*, “Low-Cost Facile Fabrication of Flexible Transparent Copper Electrodes by Nanosecond Laser Ablation,” *Adv. Mater.*, vol. 27, no. 17, pp. 2762–2767, May 2015, doi: 10.1002/adma.201500098.
[16] Q. Tong, “Direct laser writing of polymeric and metallic nanostructures via optically induced local thermal effect,” 2016.
[17] O. Bouvard *et al.*, “Mobile communication through insulating windows: a new type of low emissivity coating,” *Energy Procedia*, vol. 122, pp. 781–786, Sep. 2017, doi: 10.1016/j.egypro.2017.07.396.
[18] L. Burnier *et al.*, “Energy saving glazing with a wide band-pass FSS allowing mobile communication: up-scaling and characterisation,” *IET Microw. Antennas Amp Propag.*, vol. 11, no. 10, pp. 1449–1455, May 2017, doi: 10.1049/iet-map.2016.0685.
[19] T. Mitteramskogler *et al.*, “Fabrication of nanoparticles for biosensing using UV-NIL and lift-off,” in *34th European Mask and Lithography Conference*, Sep. 2018, vol. 10775, p. 107750Y. doi: 10.1117/12.2323700.
[20] M. Lagier, A. Bertinotti, O. Bouvard, L. Burnier, and A. Schüler, “Optical properties of in vacuo lithiated nanoporous WO3:Mo thin films as determined by spectroscopic ellipsometry,” *Opt. Mater.*, vol. 117, p. 111091, Jul. 2021, doi: 10.1016/j.optmat.2021.111091.

10 Appendix

- Confidential Report